Natriuretic Peptide Receptor A as a Novel Anticancer Target

Xiaoyuan Kong,[1] Xiaoqin Wang,[1,5] Weidong Xu,[1,4] Sumita Behera,[4] Gary Hellermann,[1] Arun Kumar,[1] Richard F. Lockey,[1,3] Subhra Mohapatra,[2,3] and Shyam S. Mohapatra[1,3]

[1]Joy McCann Culverhouse Airway Disease and Nanomedicine Research Center, Allergy and Immunology Division, [2]Endocrinology Division, Department of Internal Medicine, University of South Florida College of Medicine; [3]James A. Haley VA Hospital; [4]Transgenex Nanobiotech Inc., Tampa, Florida; and [5]Clinical Laboratory Center of First Affiliated Hospital, Xi'an Jiaotong University College of Medicine, Xi'an, China

Abstract

The receptor for atrial natriuretic peptide (ANP), natriuretic peptide receptor A (NPRA), is expressed in cancer cells, and natriuretic peptides have been implicated in cancers. However, the direct role of NPRA signaling in tumorigenesis remains elusive. Here, we report that NPRA expression and signaling is important for tumor growth. NPRA-deficient mice showed significantly reduced antigen-induced pulmonary inflammation. NPRA deficiency also substantially protected C57BL/6 mice from lung, skin, and ovarian cancers. Furthermore, a nanoparticle-formulated interfering RNA for NPRA attenuated B16 melanoma tumors in mice. Ectopic expression of a plasmid encoding NP73-102, the NH_2-terminal peptide of the ANP prohormone, which down-regulates NPRA expression, also suppressed lung metastasis of A549 cells in nude mice and tumorigenesis of Line 1 cells in immunocompetent BALB/c mice. The antitumor activity of NP73-102 was in part attributed to apoptosis of tumor cells. Western blot and immunohistochemistry staining indicated that the transcription factor, nuclear factor-κB, was inactivated, whereas the level of tumor suppressor retinoblastoma protein was up-regulated in the lungs of NPRA-deficient mice. Furthermore, expression of vascular endothelial growth factor was down-regulated in the lungs of NPRA-deficient mice compared with that in wild-type mice. These results suggest that NPRA is involved in tumor angiogenesis and represents a new target for cancer therapy. [Cancer Res 2008;68(1):249–56]

Introduction

Atrial natriuretic peptide (ANP), comprising the COOH-terminal amino acid residues 99 to 126 of the ANP prohormone, has been extensively studied for its functions in relation to blood pressure regulation (1–8). Its receptor, natriuretic peptide receptor A (NPRA), is expressed on cells in many different tissues of various organ systems and signals through guanylyl cyclase. Both ANP and brain natriuretic peptide (BNP) signal through NPRA by increasing cyclic guanosine 3′,5′-monophosphate (cGMP) and activating cGMP-dependent protein kinase (PKG). Activated PKG in turn up-regulates expression of genes encoding ion transporters and transcription factors, which together affect cell growth, apoptosis, proliferation, and inflammation (9–11).

Inflammation is an important feature of lung cancers. Alveolar macrophages from lung cancer patients secrete more proinflammatory cytokines, especially interleukin (IL)-6 and IL-1β, after lipopolysaccharide stimulation than those from persons with nonmalignant disease (12). Increased IL-6 in lung cancer patients enhances the acute phase response and is correlated with poor nutritional status and lowered survival (13). Both ANP and NPRA are expressed by lung cancer cells, and oversecretion of ANP has been linked with hyponatremia (14–16). However, little is known about the effects of NPRA signaling on inflammation and cancer progression. In addition, metastatic melanoma cells produce higher levels of cGMP in response to natriuretic peptides than other cell types, and ANP may contribute to local inflammation in the origin of metastatic melanoma (17). ANP possesses some topological similarity with melanin-concentrating hormone (12). Furthermore, the ANP gene, located on chromosome 1p36, is considered a candidate gene for melanomas (18). In some cases, natriuretic peptides including ANP have been reported to inhibit proliferation of various cancer cells and tumor growth (19). Although the mechanism of action is unclear, these peptides also decrease expression of NPRA. However, a direct role for NPRA in tumorigenesis has not been investigated thus far.

Previously, we reported that an NH_2-terminal ANP prohormone peptide comprising residues 73 to 102 (NP73-102) significantly inhibits activation of several proinflammatory transcription factors, including nuclear factor-κB (NF-κB), activator protein 1 and Erk-1,2, in human bronchial epithelial adenocarcinoma A549 cells (20, 21). Because these transcription factors augment the local inflammatory milieu, it was reasoned that NPRA signaling plays a role in and promotes tumorigenesis. By corollary, blocking NPRA signaling would attenuate tumorigenesis and development of cancers. In this study, we tested tumorigenesis in mice that are deficient in NPRA and those exhibiting attenuated expression of NPRA via treatment with nanoparticles conjugated with siNPRA or pNP73-102. The results show that NPRA attenuation or deficiency protects from tumorigenesis in lung and ovarian cancers and melanomas by several mechanisms, including decreasing local inflammation, inducing the expression of tumor suppressive gene *Rb*, and blocking vascular endothelial growth factor (VEGF) expression.

Materials and Methods

Cell lines. The mouse Lewis lung carcinoma LLC1 cell line, B16F10.9 melanoma cells, the type II alveolar epithelial adenocarcinoma cell line A549, and the normal human lung fibroblast cell line IMR 90 were purchased from American Type Culture Collection. Human prostate cancer cells PC3 and DU145 were kindly provided by Dr. Wenlong Bai in the University of South Florida, Tampa, Florida; mouse ovarian cancer cell line, ID8, was kindly provided by Dr. Janat-Amsbury (Baylor College of Medicine, Waco, TX). Both A549 and IMR 90 were grown in Earle's modified Eagle's medium supplemented with 10% fetal bovine serum (FBS) at 37°C in a 5%

Note: X. Kong and X. Wang contributed equally to this work.

Requests for reprints: Shyam S. Mohapatra, University of South Florida College of Medicine, Tampa, FL 33612. E-mail: smohapat@health.usf.edu or Subhra Mohapatra, Endocrinology Division, University of South Florida College of Medicine, Tampa, FL 33612. Phone: 813-974-4127; E-mail: smohapa2@health.usf.edu.

doi:10.1158/0008-5472.CAN-07-3086

CO_2 incubator. LLC1, ID8, and B16F10.9 cells were grown in DMEM supplemented with 10% FBS.

Animals. Female 8- to 10-week-old BALB/c mice were purchased from Jackson Laboratory. Female nude mice and C57BL/6 mice were from National Cancer Institute. C57BL/6 NPRA$^{-/-}$ (deficient in natriuretic peptide receptor A) mice were kindly provided by Dr. William Gower (Veterans Affairs Medical Center, Tampa, Florida). All mice were maintained in a pathogen-free environment and all procedures were reviewed and approved by the University of South Florida Institutional Animal Care and Use Committee.

Plasmid constructs and transfection. All plasmids used in this study were constructed using the pVAX expression vector (Invitrogen). The pNP73-102 plasmid encodes the natriuretic peptide sequence, amino acids 73 to 102, of the atrial natriuretic prohormone NH_2-terminal fragment. In some experiments, the NP73-102 sequence was fused to the FLAG sequence to allow antibody detection of NP73-120 expression in lung sections. An anti-NPRA small interfering RNA plasmid (siNPRA) was constructed as previously described. A549 cells were transfected with plasmids using Lipofectamine 2000 (Invitrogen) according to manufacturer's instructions.

Preparation of plasmid nanoparticles and administration to mice. Plasmids pNP73-102 and pVAX1 were encapsulated in chitosan nanoparticles (25 μg of plasmid plus 125 μg of chitosan). Plasmids dissolved in 25 mmol/L Na_2SO_4 and chitosan (Vanson) dissolved in 25 mmol/L Na acetate (pH 5.4; final concentration, 0.02%) were heated separately for 10 min at 55°C. After heating, the chitosan and DNA were mixed, vortexed vigorously for 20 to 30 s, and stored at room temperature until use. Plasmid nanoparticles were given to lightly anesthetized mice in the form of nose drops in a volume of 50 μL, using a pipetter with the tip inserted into the nostril.

Injection of mice with tumor cells. For s.c. challenge with LLC1, ID8, and B16F10.9 cells, cells were grown in DMEM and washed with PBS and then resuspended in PBS at 2×10^7 cells per mL for both LLC1 and ID8 or at 3×10^6 cells per mL for B16F10.9. Two groups of mice ($n = 8$ or 12 per group) were tested: wild-type C57BL/6 and C57BL/6 NPRA-deficient mice. Animals were injected s.c. with 100 μL of suspended cancer cells in the right flank. Tumor sizes were measured regularly, and the tumors were removed and weighed at the end of experiment. For the A549/nude mouse model, two groups of nude mice ($n = 4$ per group) were given 5×10^6 A549 cells by i.v. injection and treated intranasally with 25 μg of pNP73-102 or pVAX1 control nanoparticles weekly. Three weeks later, mice were sacrificed and lung sections were stained with H&E and examined for tumor nodules. Lung sections were also stained with antibodies to cyclin B and phospho-Bad. For the Line 1/BALB/c mouse model, 25 μg of pNP73-102 or pVAX1 control nanoparticles was injected i.p. into two groups of BALB/c mice ($n = 4$ per group) on days 1 and 3. A week later, these mice were injected s.c. with 10^5 Line 1 lung adenocarcinoma cells in the right flanks. Additional treatment with pNP73-102 or pVAX1 nanoparticles was continued at weekly intervals from week 2. A third group of four mice received only Line 1 cells as control. In each set of experiments, the mice were sacrificed on day 40 and their tumor burden was determined based on tumor size (measured by digital caliper) and weight.

Western blots. A549 cells were harvested and resuspended in lysis buffer containing 50 mmol/L HEPES, 150 mmol/L NaCl, 1 mmol/L EDTA, 1 mmol/L EGTA, 10% glycerol, 0.5% NP40, 0.1 mmol/L phenylmethylsulfonyl fluoride, 2.5 μg/mL leupeptin, 0.5 mmol/L NaF, and 0.1 mmol/L sodium vanadate to extract whole-cell protein. Fifty micrograms of protein was separated by SDS-PAGE on a 10% polyacrylamide gel and transferred onto nitrocellulose membranes. Western immunoblots were performed according to the manufacturer's instructions (Cell Signaling Technology). Antibodies against NF-κB p65, phosphorylated NF-κB p65 (Ser^{536}), and phosphorylated retinoblastoma protein (pRb) were purchased from Cell Signaling; antibodies against VEGF or NPRA were ordered from Santa Cruz Biotechonology.

Knockdown of NPRA expression with siNPRA. Small interfering RNA constructs that targeted the NPRA transcript were prepared and tested for effectiveness by immunoblot for NPRA levels in cells transfected with the vector-driven siNPRA (psiNPRA) plasmid. The siNPRA9 construct was selected for tumorigenesis experiments. B16 melanoma cells (1.5×10^5) were injected s.c. into 12-week-old female C57BL/6 mice. The mice were then given intranasal suspensions of 33 μg of siNPRA oligos, siNPRA plasmid, or scrambled oligos encapsulated in chitosan nanoparticles at a ratio of 1:2.5. In experiments to determine the efficacy of topical siNPRA, chitosan nanoparticles containing siNPRA plasmid or oligos were mixed with cream and applied to the injection area. Cream-containing siNPRA nanoparticles was applied twice a week and the control group received cream only. Mice were sacrificed on day 22 and tumors were removed and weighed.

Apoptosis assays. A549 or normal IMR90 cells were grown in 6-well plates and transfected with pVAX1 or pNP73-102. Forty-eight hours after transfection, cells were examined for apoptosis by terminal deoxynucleotidyl transferase-mediated dUTP-biotin end labeling (TUNEL) assay, and poly-ADP ribose polymerase (PARP) cleavage by Western blotting. In the TUNEL assay, cell nuclei were stained with 4′,6-diamidino-2-phenylindole (DAPI) to enable counting of total cell numbers and determination of the percentage of TUNEL-positive cells. For the PARP cleavage, whole-cell protein was isolated and equal amounts were Western blotted using an antibody to PARP. Experiments were done in duplicate.

Statistics. The number of mice used in each test group was a minimum of 4 and usually 8 or 12. Experiments were repeated at least once, and measurements were expressed as means ± SE or SD. Comparisons of groups were done using a two-tailed Student's t test.

Results

NPRA deficiency decreases lung inflammation. To determine whether the ANP-NPRA pathway contributes to pulmonary inflammation, we compared the lungs of mice deficient in NPRA (NPRA$^{-/-}$) with those of wild-type mice after immunization with ovalbumin i.p. and subsequent challenge with ovalbumin intranasally. C57BL/6 wild-type mice ($n = 8$) showed substantially higher inflammation, blocked airways, and goblet cell metaplasia than did NPRA$^{-/-}$ mice (Fig. 1). Bronchoalveolar lavage (BAL) fluid from NPRA$^{-/-}$ mice had significant reduced levels of the inflammatory cytokines IL-4, IL-5, and IL-6 relative to those in wild-type mice (data not shown).

NPRA deficiency protects mice against lung, skin, and ovarian cancers. Recent research suggests that alterations in the lung microenvironment caused by inflammation are related to carcinogenesis (22). Proinflammatory conditions, especially those related to chronic pulmonary irritation, may contribute to the development of lung cancer (23). A direct link between inflammation and lung tumors can be seen in the particle-induced lung cancer murine model (24). Integral to the involvement of inflammation in the development of lung cancer is the profile of

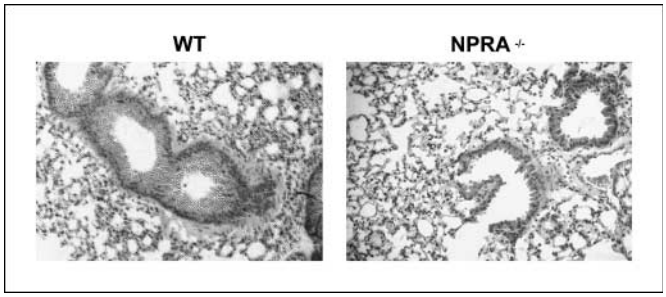

Figure 1. NPRA expression and signaling is involved in lung inflammation. NPRA$^{-/-}$ mice exhibit reduced lung inflammation. Wild-type C57BL/6 and NPRA$^{-/-}$ mice ($n = 4$) were sensitized (i.p.) at day 0 and day 7 and then challenged twice with ovalbumin. Two days later, mice were sacrificed and lung sections were stained with hematoxylin/eosin.

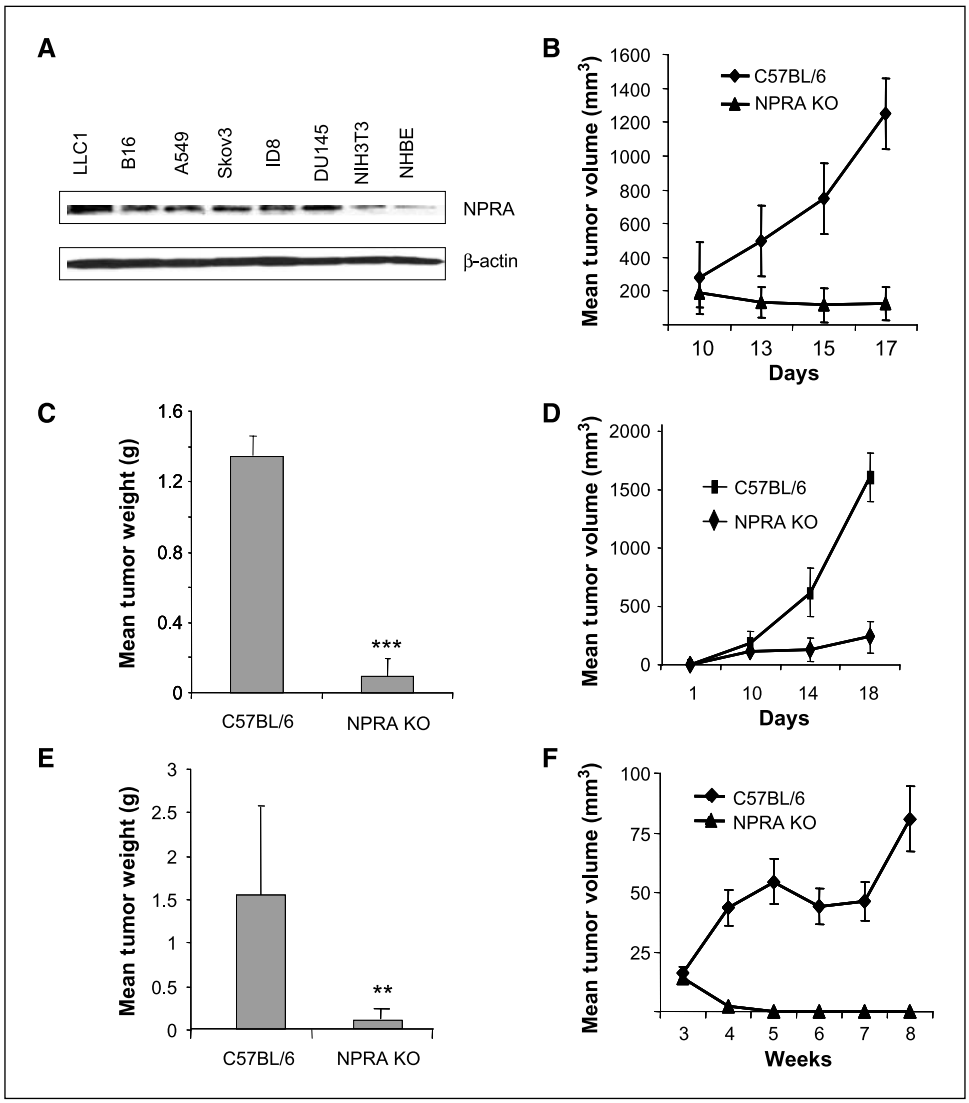

Figure 2. NPRA$^{-/-}$ mice are resistant to tumorigenesis. *A,* NPRA is overexpressed in various cancer cells compared with normal cells. Whole proteins were extracted from different cell lines and subjected to Western blot using primary antibodies against NPRA. *B* and *C,* groups of wild-type and NPRA$^{-/-}$ mice (n = 8 per group) were injected s.c. with 2×10^6 LLC1 cells. Tumor sizes (*B*) were measured on day 10, 13, 15, and 17, and tumor weights (*C*) at day 17 were compared ($P < 0.01$). *D* and *E,* groups of wild-type and NPRA$^{-/-}$ mice (n = 12) were injected s.c. with 2×10^6 B16 melanoma cells, tumor sizes (*D*) were measured on day 1, 10, 14, and 18, and tumor weights (*E*) were measured and compared at day 18 ($P < 0.01$). Data from one of the two repeated experiments is presented. *F,* groups of wild-type and NPRA$^{-/-}$ mice (n = 8) were injected s.c. with 2×10^6 mouse ovarian cancer ID8 cells and tumor sizes were measured every week after ID8 injection.

cytokines produced (25). Because ANP-NPRA signaling is involved in lung inflammation, we sought to investigate the role of the ANP-NPRA signaling pathway in the development of cancers of the lung and other organs. To illustrate the role of the ANP-NPRA signaling pathway in cancer development, we compared NPRA expression in various tumor cells and normal cells. We found that NPRA is expressed at a higher level in all tumor cells, including cells of lung carcinoma (A549 and LLC1), melanoma (B16), ovarian cancer (SKOV3 and ID8), and prostate cancer cells (DU145), compared with that in normal human bronchial epithelial cells (Fig. 2*A*).

To determine whether blockade of ANP signaling could have a protective effect against development of cancer, various C57/BL6 murine models of tumorigenesis were evaluated. Using the Lewis lung carcinoma model, C57BL/6 wild-type and NPRA$^{-/-}$ mice (n = 8 for each group) were injected s.c. with 2×10^6 LLC1 cells in the right flank. Tumors appeared within 1 week after injection, and tumor size was measured with a digital caliper beginning on day 10. The tumors in wild-type mice grew rapidly after day 10, but tumors in NPRA$^{-/-}$ mice gradually shrank. On day 17, all mice were sacrificed, and tumor sizes and weights were measured. In one of the NPRA$^{-/-}$ mice, no visible tumors were observed. Significant differences in tumor size and weight were observed between the two groups (Fig. 2*B* and *C*). As a further test of the antitumor effects of NPRA deficiency, mice were injected s.c. with B16 melanoma cells. A significant reduction in mean tumor volume, measured >18 days after B16 cell injection, and a significant decrease in tumor weight at day 18 were observed in NPRA$^{-/-}$ mice (n = 12) but not in wild-type mice (Fig. 2*D* and *E*). The potential of NPRA deficiency to inhibit the growth of ovarian cancer cells was also tested. Groups of wild-type (n = 8) and NPRA-deficient (n = 8) C57BL/6 mice were injected with 2×10^6 ID8 mouse ovarian cancer cells at day 1 and were monitored at weekly intervals for tumor growth. By week 8 after cancer cell inoculation, all mice from the wild-type group developed solid tumors, but no tumors were observed in NPRA-deficient mice (Fig. 2*F*). Again NPRA$^{-/-}$ mice exhibited a significant reduction in ovarian cancer development compared with that in wild-type mice. These results indicate that NPRA deficiency significantly protects mice from tumorigenesis and tumor progression.

Inhibition of melanoma by siNPRA nanoparticles. To further validate NPRA as a drug target for cancer therapy, we used siRNA to knock down NPRA expression in C57BL/6 mice and tested their

ability to inoculate B16 melanoma cells. To test whether nanoparticle-mediated siRNA transfer could be used for this purpose, we intratumorally injected chitosan-siGLO nanocomplexes into the PC3-induced prostate tumors in BALB/c nude mice, and siGLO was examined 48 h after injection. Fluorescence microscopy revealed that siGLO was only present in tumors when delivered in nanocomplexes but not when delivered in naked form (Fig. 3*A*). To identify the most effective siRNA, we screened several candidates and identified three that inhibited NPRA expression. HEK293-GCA cells that overexpress NPRA were transfected with one of these siNPRAs or with scrambled siNPRA (Scr), and cell lysates were examined at 48 h for NPRA expression by Western blotting. As shown in Fig. 3*B*, siNPRA decreased NPRA expression by about 60%. Because NPRA-deficient C57BL/6 mice may have abnormalities that make them resistant to tumor development, wild-type mice were injected with 3×10^5 B16F10.9 melanoma cells and were then treated twice a week with a cream containing either synthetic siNPRA, psiNPRA, or Scr, respectively, for four consecutive weeks at the site of tumor cell injection. Four weeks later, tumor burden from each group was compared. A significant reductions in tumor burden was seen in mice treated with siNPRA (either with synthetic or psiNPRA) but not those given Scr (Fig. 3*C*), indicating that siNPRA can be used to treat melanomas.

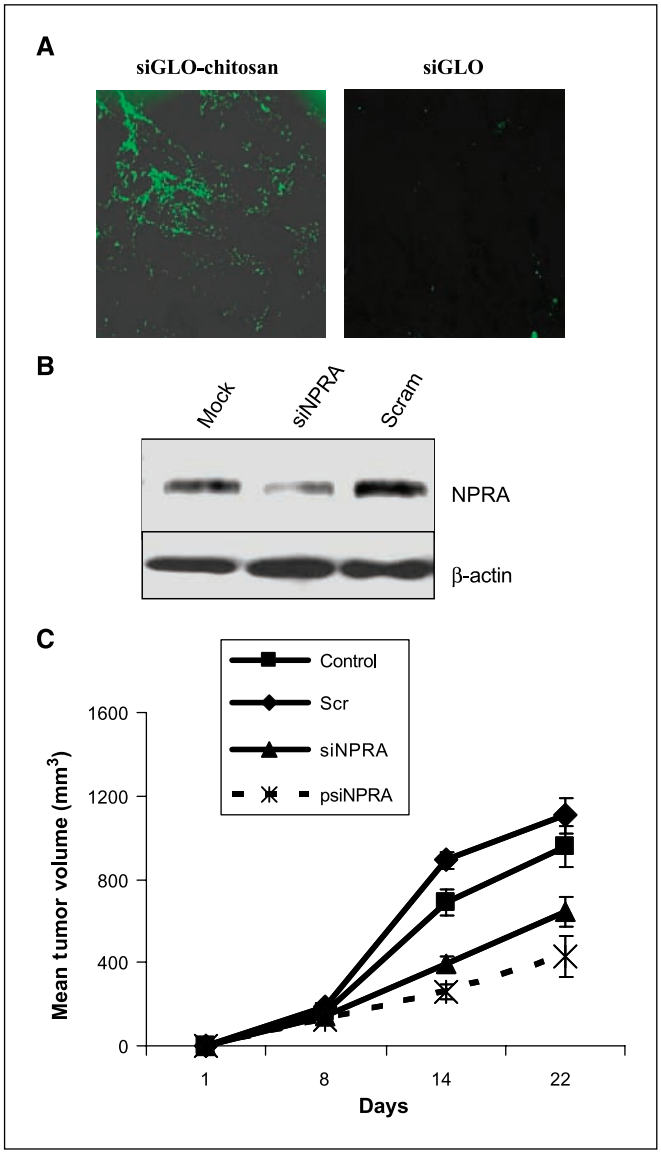

Figure 3. siNPRA nanoparticles decrease tumor burden. *A,* nanoparticle-transported siRNA, but not naked siRNA, is retained in the tumor. BALB/c nude mice injected s.c. with PC3 prostate cancer cells were treated with chitosan-siGLO nanocomplexes or naked siGLO, and tumor sections were examined after 48 h by fluorescence microscopy. *B,* inhibition of NPRA expression in HEK293-GCA cells by siNPRA. HEK293-GCA cells were untreated, transfected with siNPRA, or with scrambled siRNA. Cells were harvested 48 h after transfection. Total protein was extracted and subjected to Western blot assay with primary antibody against NPRA. *C,* B16 melanoma cells (1.5×10^5) were injected s.c. into 12-wk-old female C57BL/6 mice. These mice were then treated with synthetic siNPRA, psiNPRA, or Scr. All of these were mixed with chitosan at a ratio of 1:2.5. Mixed chitosan and plasmid or oligos were mixed again with a cream before application to the injection area. The control group was given cream only. These treatments were given twice a week. Mice were sacrificed on day 22, and tumors were removed and weighed. *Points,* mean; *bars,* SD; $n = 16$; $P < 0.01$.

Suppression of lung cancer tumorigenesis by NP73-102 nanoparticles. NP73-102 decreases activation of several transcription factors, including NF-κB that promote tumorigenesis. To test whether overexpression of NP73-102 affects NPRA expression *in vivo*, pregnant mice were injected i.p. with pNP73-102 or pVAX1. After 3 to 5 days, mice were sacrificed, and thymocytes were isolated from embryos. NPRA or natriuretic peptide receptor C (NPRC) levels were quantitated by flow cytometry with gating on CD4+ cells. Expression of both NPRA and NPRC in embryonic thymi was significantly reduced by pNP73-102 when compared with that in control mice injected with pVAX1 (Fig. 4*A*). Because NPRA-deficient mice had reduced tumorigenicity, it was reasoned that NP73-102 might have antitumor activity, and this was evaluated *in vitro* in A549 cells using a soft agar assay. A549 cells were transfected with pVAX1, pANP, or pNP73-102. The results from the soft agar assay (data not shown) indicated that cells transfected with pNP73-102 exhibited significantly decreased colony formation compared with that of nontransfected cells or cells transfected with pVAX1. To test whether overexpression of a plasmid DNA encoding NP73-102 could express the peptide *in vivo* in the lung, a pNP73-102-FLAG was constructed, in which NP73-102 was fused to a FLAG epitope to verify expression of NP73-102 in lung cells. The pNP73-102-FLAG, encapsulated in chitosan nanoparticles, was given to mice intranasally, and 24 h later, a BAL was performed. BAL cells were stained with anti-FLAG antibody, and substantial numbers of cells expressing NP73-102-FLAG were observed (Fig. 4*B*).

To determine whether intranasal NP73-102 nanoparticle administration abrogates metastasis in mice, 12 nude mice were separated into three groups ($n = 4$ per group). Mice were given 5×10^6 A549 cells i.v. and weekly instillations of PBS (control) or nanoparticles carrying pNP73-102 or pVAX1. Three weeks later, mice were sacrificed and lung sections were stained with H&E and examined for lung nodules. Control animals receiving only PBS showed nodules and tumors, whereas the NP73-102–treated group had no tumors (Fig. 4*C*). Additionally, the lung sections were stained with antibodies to promitotic cyclin B and to antiapoptotic phospho-Bad (biomarkers of lung tumors), and mice treated with NP73-102 did not show any staining for cyclin B or phospho-Bad (Fig. 4*D*). To test whether NP73-102 nanoparticles could attenuate tumor burden in an immunocompetent mouse lung cancer model, BALB/c mice (4–6 week old female; $n = 3$ to 4 per group) were given pNP73-102 (25 μg/mouse; i.p.) on days 1 and 3 and then s.c. injected with 10^5 Line 1 cells in the right flank on day 7. Thereafter, mice were i.p. injected with pNP73-102 nanoparticles at weekly intervals. The mice were sacrificed on day 40, and the size and weight of tumors was measured. The results show that the tumor

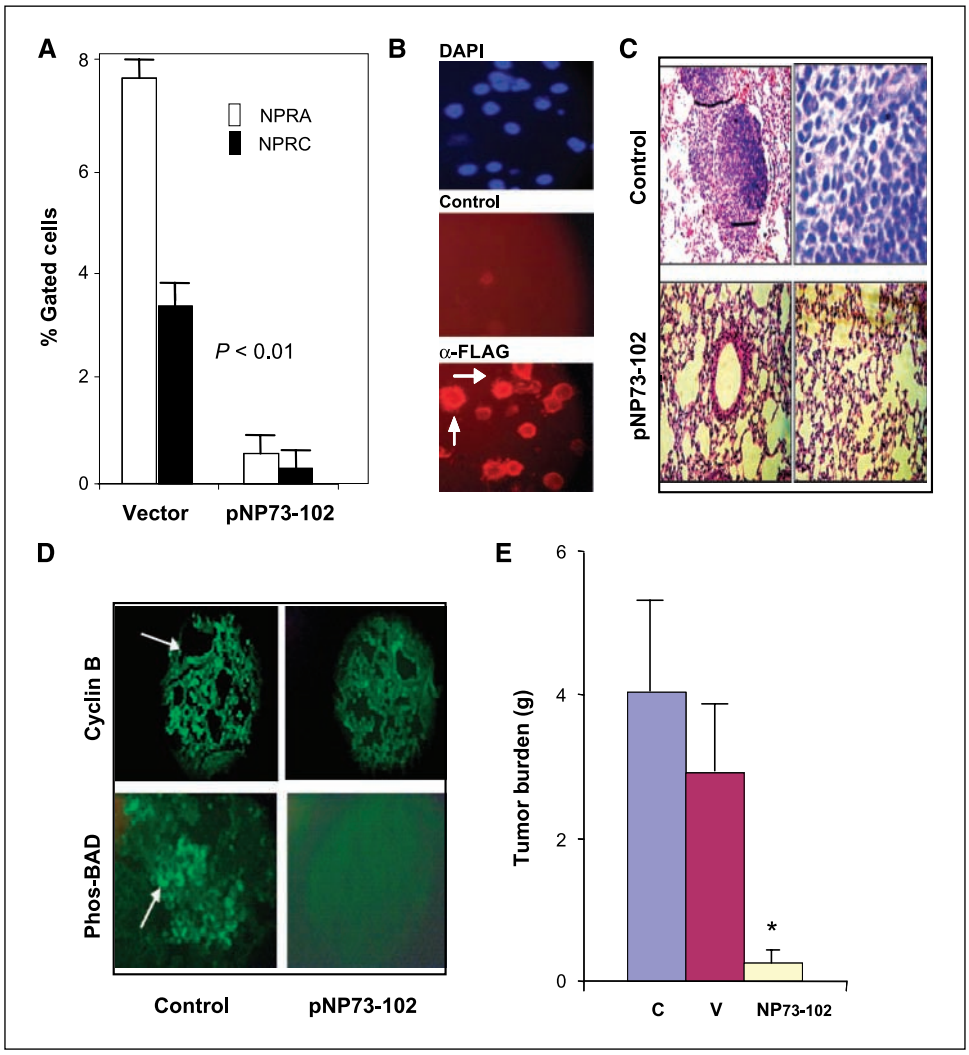

Figure 4. pNP73-102 nanoparticles decrease NPRA expression and lung tumor development. *A,* modulation of NPRA expression by NP73-102 *in vivo*. Pregnant (12 d) mice were injected with pNP73-102 or pVAX1 (control vector). After 1 d, mice were sacrificed and the expression of NPRA and NPRC was measured by flow cytometry in CD4+-gated cells. *B,* expression of NP73-102-FLAG in BAL cells after intranasal administration of pNP-73-102-FLAG peptide. After 24 h, BAL cells were stained with either second antibody as control or anti-FLAG antibody and then with DAPI. *C,* nude mice were given 5×10^6 A549 cells i.v. and weekly intranasal doses of nanoparticles carrying either empty plasmid (control) or pNP73-102. Three weeks later, mice were sacrificed, and lung sections were stained with hematoxylin/eosin and examined for tumor nodules. *D,* lung sections were also stained with antibodies to cyclin B and phosphoBad. *E,* BALB/c mice were given pNP73-102 on days 1 and 3 and injected s.c. with 10^5 Line 1 cells on day 7. From then on, the mice were given pNP73-102 at weekly intervals. Mice were sacrificed on day 40 and their tumor burden was determined based on size and weight. Control group (*C*) received no treatment and a second control group (*V*) received nanoparticles containing pVAX. *Columns,* mean; *bars,* SD; $n = 16$; $P < 0.01$.

burden in pNP73-102–treated mice was significantly reduced compared with the tumor burden in those treated with PBS or pVAX1 control vector (Fig. 4*E*).

NP73-102 induces apoptosis of A549 adenocarcinoma and B16 melanoma cells. To verify whether antitumor effects of pNP73-102 can be attributed to loss of cell viability, A549 and normal WI-138 cells were examined for apoptosis by TUNEL assay after 24 h of transfection. The results indicated that ~80% of A549 cells transfected with pNP73-102 underwent apoptosis compared with only 10% of WI-138 cells (Fig. 5*A*). In addition, more A549 cells were observed to be TUNEL-positive when treated with pNP73-102 than were observed among cells treated with pVAX1 (data not shown). Apoptosis was further confirmed by examining for the cleavage of the caspase 3 substrates, PARP, by Western blotting. A549 cells transfected with pNP73-102 showed more cleaved PARP than controls (Fig. 5*B*). A microarray analysis of gene expression of A549 cells after transfection with either pVAX1 or pNP73-102 was performed. The results showed that pNP73-102 significantly altered, both positively and negatively, the expression of a number of genes (data not shown). The up-regulated genes were predominantly from the family of IFN-regulated genes or related signal transduction pathways. Similarly, the down-regulated genes included some involved in inflammation, suggesting that NP73-102 has anti-inflammatory, in addition to antitumor, properties. To determine whether apoptosis induction was the dominant explanation for the antitumor activity of pNP73-102, we tested the effect of over-expressing pNP73-102 in B16 melanoma and normal NIH3T3 cells. The results showed significant apoptosis of B16 cells as measured by flow cytometry assay but not of the normal cells (data not shown). Also, significantly more B16 cells were observed to be TUNEL-positive when they were treated with pNP73-102 compared with the number observed among cells treated with pVAX1 (Fig. 5*C*). These results indicated that a decrease in ANP-NPRA signaling may result in the induction of apoptosis in cancer cells but not in normal cells.

NF-κB and pRb are involved in tumor suppression in NPRA-deficient mice. Activation of the NF-κB pathway enhances tumor development and may act primarily during the late stages of tumorigenesis. To determine whether the lungs of $NPRA^{-/-}$ mice differ in NF-κB activation when compared with wild-type mice, we examined the lung extracts for signs of NF-κB activation through Western blot. Whole proteins were extracted from the lungs of wild-type and $NPRA^{-/-}$ mice and then probed using primary antibodies against p50, p65, phospho-p50, and phospho-p65. No significant difference in NF-κB expression in the lungs was observed between wild-type and $NPRA^{-/-}$ mice (Fig. 5*D*). However, the level of the activated form of NF-κB, phospho-NF-κB (both

phospho-p65 and phospho-p50), was decreased in NPRA$^{-/-}$ mice (Fig. 5*D*). These results suggest that the role of NPRA in lung inflammation may involve NF-κB activation.

We then tested whether pRb, the protein product of the retinoblastoma cancer suppressor gene, is involved in the suppression of tumor growth in NPRA$^{-/-}$ mice. pRb and other retinoblastoma family members, such as pRb2/p130 and p107, are involved in controlling four major cellular processes of growth arrest, apoptosis, differentiation, and angiogenesis. Inactivation of pRb has been shown to play an important role in the pathogenesis of human cancers. We compared the expression of pRb in the lungs of wild-type C57BL/6 and NPRA$^{-/-}$ mice by immunohistochemistry analysis. It was revealed that NPRA deficiency induced overexpression of pRb (Fig. 5*E*). In addition, expression of VEGF, which is important in angiogenesis, was decreased in the lungs of NPRA-deficient mice, as observed by Western blotting (Fig. 5*D*). The differential expression of pRb and VEGF may help to explain why several types of cancer were inhibited in NPRA$^{-/-}$ mice but not in wild-type mice. We also compared the expression of another major tumor suppressor gene, *p53*, in the lungs of wild-type and NPRA$^{-/-}$ mice through Western blot analysis, and no significant difference was observed (data not shown).

Other mechanistic studies were performed to understand why lung tumor growth was inhibited in NPRA$^{-/-}$ mice by comparing gene expression in the lungs of wild-type and NPRA$^{-/-}$ mice. Superarray analysis revealed that the expression of several genes, such as hexokinase 2, glycogen synthase 1, and matrix metallopeptidase 10 were down-regulated from about 4- to 17-fold in the lungs of NPRA$^{-/-}$ mice. Interestingly, the expression of cellular retinol binding protein 1 was up-regulated about 5.5-fold in the lungs of NPRA$^{-/-}$ mice.

Discussion

A significant finding of this study is the demonstration that signaling through NPRA, which is the receptor for ANP and BNP, plays a pivotal role in tumorigenesis. As a key signaling molecule, NPRA produces the second messenger cGMP and activates PKG. PKG activation in turn activates ion transporters and transcription factors, which together affect cell growth and proliferation,

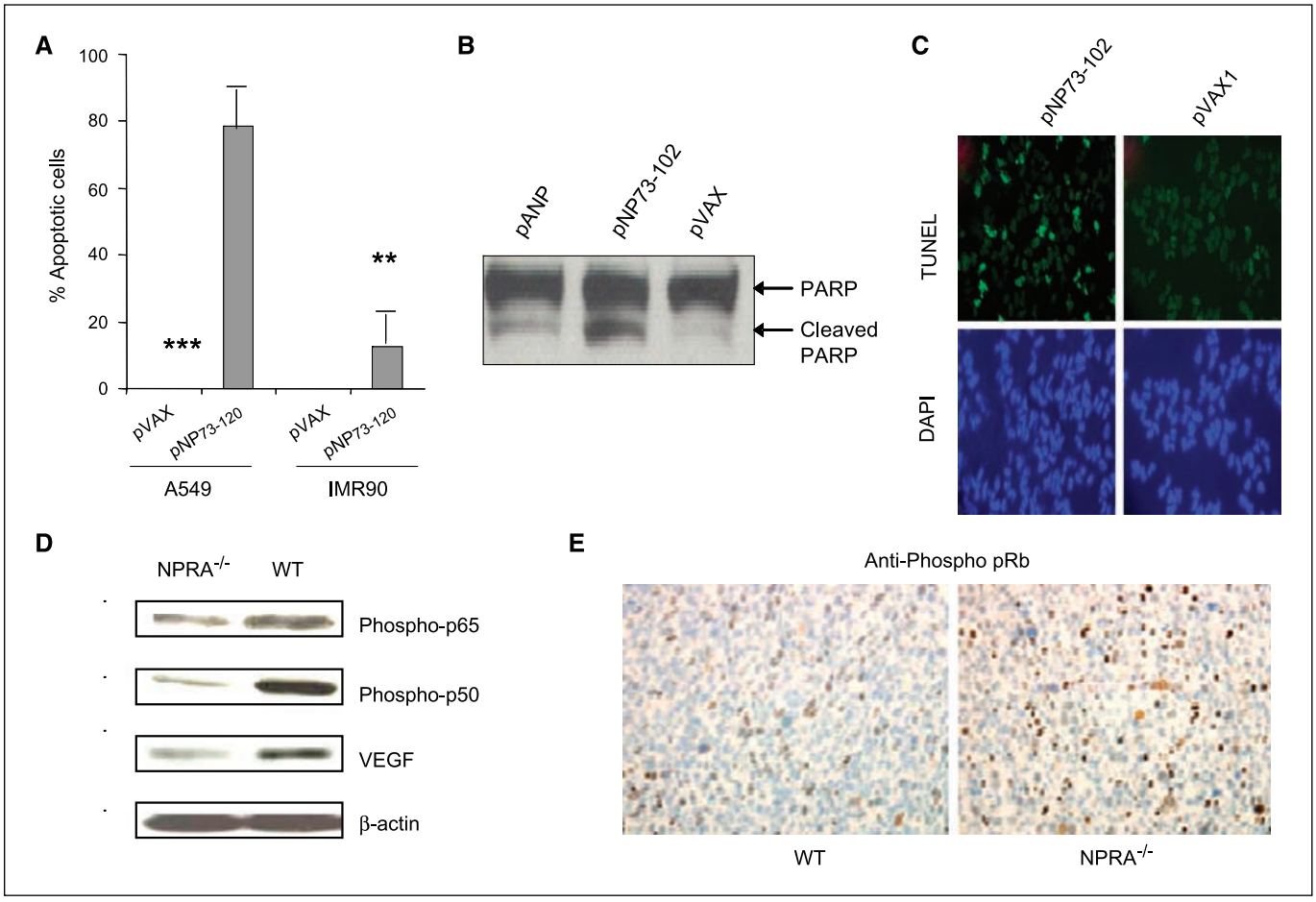

Figure 5. Mechanism of tumor suppression by NP73-102 and NPRA deficiency. *A* to *C,* NP73-102–induced apoptosis in cancer cells. *A,* pNP73-102 does not induce apoptosis of normal cells, only A549 cancer cells. A549 adenocarcinoma or normal IMR90 cells were transfected with pVAX1 or pNP73-102. Cells were stained by TUNEL assay and nuclei were visualized with DAPI. TUNEL-positive cells were counted under a fluorescence microscope, and the number was expressed as percent TUNEL-positive cells relative to the total number of cells; less NPRA-positive cells were detected after pNP73-102 treatment ($P < 0.01$). *B,* proteins were isolated and equal amounts were Western blotted using an antibody to PARP. *C,* B16 melanoma cells were transfected with pVAX or pNP73-120, respectively. TUNEL-positive cells were counted under a fluorescence microscope and the number was expressed as percent TUNEL-positive cells relative to the total number of cells. *D* and *E,* NF-κB and pRb are involved in tumor suppression in NPRA-deficient mice. *D,* NPRA deficiency inactivated NF-κB and down-regulated VEGF expression. Whole proteins were extracted from lungs of wild-type and NPRA$^{-/-}$ mice and then subjected to Western blot using primary antibodies against NF-κB, phospho-NF-κB, and VEGF. *E,* differential expression of pRb in the lungs of wild-type and NPRA$^{-/-}$ mice. Lungs of wild-type and NPRA$^{-/-}$ C57BL/6 mice ($n = 4$) were sectioned and examined for pRb expression using phospho-pRb antibody in immunohistologic staining. *Arrows,* phospho-pRb–positive cells.

apoptosis, and inflammation. The finding that NPRA$^{-/-}$ mice showed reduced lung inflammation indicates that ANP-NPRA signaling is involved in the inflammatory process. These data are supported by an observed decrease in eosinophil numbers and in Th1-like and Th2-like cytokines in BAL fluid from NPRA$^{-/-}$ mice compared with levels in wild-type mice (data not shown). These results show that ANP-NPRA signaling promotes inflammation in rodent models.

To test the hypothesis that the increased inflammation contributes to the genesis of cancer, three different cancer models were investigated in C57BL/6 wild-type mice and NPRA$^{-/-}$ mice. These include the Lewis-lung carcinoma model, the B16-induced melanoma model, and the ID8-induced spontaneous model for ovarian cancer. In all these models, the NPRA$^{-/-}$ mice showed little or no tumor growth compared with wild-type mice. ANP has been reported to possess anticancer properties (19), and our data are consistent with this because ANP overexpression is known to decrease NPRA levels in cells (26) presumably by feedback inhibition. Natriuretic peptides, such as KP and VD (27, 28), have also been reported to inhibit cancer cell proliferation and have shown anticancer activities, although the mechanism of their inhibition is not known. Because these peptides down-regulate NPRA expression, it is likely that these peptides may also function by regulating NPRA signaling; therefore, NPRA may be considered a target for cancer treatment.

To further validate NPRA as a drug target for cancer therapy, we used siRNA to knock down NPRA expression in immunocompetent C57BL/6 mice. Plasmids were designed that induce degradation of NPRA transcripts and block expression of NPRA. To protect the siNPRA plasmid from degradation and to facilitate its entry into tumor cells, the DNA was complexed with chitosan nanoparticles, and this represents a significant improvement in the delivery of siRNA to tumor cells. In a B16 melanoma model, mice treated with siNPRA nanoparticles showed a significant reduction in tumors compared with those of mice given Scr as a control. To further test this approach, siNPRA was used to treat mice injected with ovarian cancer cells. Again, the growth of the tumor xenograft was inhibited significantly in these mice (data not shown). Treatment with siNPRA, however, was not as complete as seen in NPRA$^{-/-}$ mice; this could be because siRNA knockdown was not complete or that a large enough dose of siNPRA was not used. Nonetheless, these studies have confirmed the potential of using NPRA inhibitors as an anticancer agent.

The finding that pNP73-102 inhibits NPRA expression prompted us to examine its role in treating lung cancer using chitosan nanoparticle–based intranasal gene therapy. A549 cells injected into BALB/c nude mice induced lung micrometastasis in the control mice but not in pNP73-102–treated mice. The location of the lung tumors, as indicated by cyclin B and phospho-BAD biomarkers, was in agreement with the tissue staining data. In addition, tests of spontaneous lung tumorigenesis induced with Line 1 cells in immunocompetent BALB/c mice showed that treatment with pNP73-102 significantly reduced tumors compared with those observed after treatment with pVAX vector alone. These findings confirm the potential utility of pNP73-102 for the treatment of lung cancers. Although the mechanism of tumor inhibition by NP73-102 is unknown, the evidence that pNP73-102 significantly decreases the expression of NPRA suggests that this may be the explanation for its antitumor effect.

Localized inflammation involving proinflammatory transcription factors such as NF-κB has been implicated in the development of cancers (29). Several groups have reported in mouse models of intestinal (30), liver (31), and mammary (32) cancer that activation of the NF-κB pathway enhances tumor development and may act primarily in the late stages of tumorigenesis. Many tumor cell lines show constitutive activation of NF-κB, but there has been conflicting evidence as to whether it promotes or inhibits tumorigenesis. Several groups have reported that activation of the NF-κB pathway enhances tumor development and may act primarily in the late stages of tumorigenesis in mouse models of intestinal, liver, and mammary cancer. Inhibition of NF-κB signaling uniformly suppressed tumor development but, depending on the model studied, this salutary effect was attributed to an increase in tumor cell apoptosis, reduced expression of tumor cell growth factors supplied by surrounding stromal cells, or abrogation of a tumor cell dedifferentiation program that is critical for tumor invasion/metastasis (33–40). The demonstration that pNP73-102 inhibited activation of NF-κB and that NF-κB activation was reduced in the lungs of NPRA$^{-/-}$ mice could represent another additional mechanism underlying its anticancer activity. Moreover, we observed less lung inflammation in NPRA$^{-/-}$ mice than was observed in wild-type counterparts when they were challenged by ovalbumin in an asthma model. The results presented here provide evidence of a critical role for natriuretic peptides and NPRA signaling in many different cancers, including lung cancer, ovarian cancer, and melanoma. Interestingly, NF-κB binding activity was 4-fold greater in the nuclear extracts of NPRA$^{-/-}$ mouse hearts than in those of wild-type mouse hearts (41). Reduced inflammation was also reported in the hearts of NPRA$^{-/-}$ mice (42). Further investigation is needed to understand the differential regulation of NF-κB activity and inflammation in the mouse lung and heart after loss of the NPRA gene.

To identify the mechanism by which NPRA deficiency suppresses the growth of several types of tumors, we analyzed the expression of tumor suppressor genes, including p53 and pRb. Tumor suppressor genes participate in a variety of critical and highly conserved cell functions, including regulation of the cell cycle and apoptosis, differentiation, surveillance of genomic integrity and repair of DNA errors, signal transduction, and cell adhesion. The *p53* gene is the best known, but other tumor suppressor genes of interest include the retinoblastoma gene (*pRb*), *PTEN, p16, nm23*, and *maspin* (42). We found that there was no significant difference in the level of p53 in the lungs of NPRA$^{-/-}$ and wild-type mice. However, the phosphorylation of pRb was up-regulated in the lungs of NPRA$^{-/-}$ mice, as indicated by Western blot assays. pRb plays a critical role in the control of cell proliferation and in DNA damage checkpoints and inhibits cell cycle progression through interactions with the E2F family of transcription factors. In tumorigenesis, loss of Rb function is an important event caused by gene mutation, promoter hypermethylation, deregulation of Rb phosphorylation, and viral protein sequestration. Dysfunctional pRb has been reported in many different types of tumors, including those of the eye, bone, lung, breast, and genitourinary system. In our investigation, we found that NPRA deficiency did not affect pRb expression but did up-regulate pRb phosphorylation.

The Rb gene family is also involved in tumor angiogenesis (43). Angiogenesis represents a fundamental step in tumor progression and metastasis. The induction of vasculature is important for tumor growth because it ensures an adequate supply of oxygen and metabolites to the tumor. pRb regulates the expression of proangiogenic and antiangiogenic factors, such as the VEGF, through an E2F-dependent mechanism. Some natural and syn-

thetic compounds show their antiangiogenic activity through a mechanism of action involving pRb. Consistent with the activation of pRb in the lungs of NPRA$^{-/-}$ mice, the expression of VEGF was down-regulated in NPRA$^{-/-}$ mice when compared with that in wild-type mice. This indicated that angiogenesis was attenuated in NPRA$^{-/-}$ mice, which may contribute to the suppression of tumor growth in NPRA$^{-/-}$ mice. Although we have only showed that the differential expression of pRb and VEGF may play an important role in the mechanism of tumor suppression in NPRA$^{-/-}$ mice (43), additional studies are under way to determine which of the several signal transduction pathways in which NPRA is involved are important for the antitumor effect. Because clinical studies of the natriuretic peptides have not indicated any incompatibility reactions or toxic effects (44), we expect that combining the advantage of chitosan nanoparticles in targeted delivery of anticancer drugs with gene therapy based on the novel pNP73-102 nanoparticles or siNPRA nanoparticles may provide a safe and effective treatment for a wide range of cancers in the future.

Acknowledgments

Received 8/16/2007; accepted 10/30/2007.

Grant support: NIH (RO1-5HL71101A2), Veterans Affairs Merit Review and Career Scientist Awards, and Florida Biomedical Research Foundation Bankhead-Coley Awards (S.S. Mohapatra); Florida Department of Health James and Esther King Biomedical Research Grant (S. Mohapatra); and by the Joy McCann Culverhouse and Mabel-Ellsworth Simmons endowments to the University of South Florida Division of Allergy and Immunology.

The costs of publication of this article were defrayed in part by the payment of page charges. This article must therefore be hereby marked *advertisement* in accordance with 18 U.S.C. Section 1734 solely to indicate this fact.

References

1. Vesely DL. Atrial natriuretic hormones originating from the N-terminus of the atrial natriuretic factor prohormone. Clin Exp Pharmacol Physiol 1995;22:108–14.
2. Vesely DL. Atrial natriuretic peptides in pathophysiological diseases. Cardiovasc Res 2001;51:647–58.
3. Vesely DL. Atrial natriuretic peptide prohormone gene expression: hormones and diseases that upregulate its expression. IUBMB Life 2002;53:153–9.
4. Vesely DL, Chiou S, Douglass MA, McCormick MT, Rodriguez-Paz G, Schocken DD. Atrial natriuretic peptides negatively and positively modulate circulating endothelin in humans. Metabolism 1996;45:315–9.
5. Vesely DL, Perez-Lamboy GI, Schocken DD. Vessel dilator, long acting natriuretic peptide, and kaliuretic peptide increase circulating prostaglandin E2. Life Sci 2000;66:905–13.
6. Vesely DL, Perez-Lamboy GI, Schocken DD. Long-acting natriuretic peptide, vessel dilator, and kaliuretic peptide enhance the urinary excretion rate of β2-microglobulin. Metabolism 2000;49:1592–7.
7. Vesely DL, San Miguel GI, Hassan I, Schocken DD. Atrial natriuretic hormone, vessel dilator, long-acting natriuretic hormone, and kaliuretic hormone decrease the circulating concentrations of CRH, corticotropin, and cortisol. J Clin Endocrinol Metab 2001;86:4244–9.
8. Vesely DL, San Miguel GI, Hassan I, Schocken DD. Atrial natriuretic hormone, vessel dilator, long acting natriuretic hormone, and kaliuretic hormone decrease circulating prolactin concentrations. Horm Metab Res 2002;34:245–9.
9. Fiscus RR. Involvement of cyclic GMP and protein kinase G in the regulation of apoptosis and survival in neural cells. Neurosignals 2002;11:175–90.
10. Pedram A, Razandi M, Kehrl J, Levin ER. Natriuretic peptides inhibit G protein activation. Mediation through cross-talk between cyclic GMP-dependent protein kinase and regulators of G protein-signaling proteins. J Biol Chem 2000;275:7365–72.
11. Silberbach M, Roberts CT, Jr. Natriuretic peptide signalling: molecular and cellular pathways to growth regulation. Cell Signal 2001;13:221–31.
12. Matanic D, Beg-Zec Z, Stojanovic D, Matakoric N, Flego V, Milevoj-Ribic F. Cytokines in patients with lung cancer. Scand J Immunol 2003;57:173–8.
13. Martin J, Quiroga JA, Navas S, Pardo M, Carreno V. Modulation by biologic response modifiers of hepatitis C virus antigen-independent cytokine secretion in blood mononuclear cells. Cytokine 1999;11:267–73.
14. Bliss DP, Jr., Battey JF, Linnoila RI, Birrer MJ, Gazdar AF, Johnson BE. Expression of the atrial natriuretic factor gene in small cell lung cancer tumors and tumor cell lines. J Natl Cancer Inst 1990;82:305–10.
15. Ohsaki Y, Gross AJ, Le PT, Oie H, Johnson BE. Human small cell lung cancer cells produce brain natriuretic peptide. Oncology 1999;56:155–9.
16. Ohsaki Y, Yang HK, Le PT, Jensen RT, Johnson BE. Human small cell lung cancer cell lines express functional atrial natriuretic peptide receptors. Cancer Res 1993;53:3165–71.
17. Izumi T, Saito Y, Kishimoto I, et al. Blockade of the natriuretic peptide receptor guanylyl cyclase-A inhibits NF-κB activation and alleviates myocardial ischemia/reperfusion injury. J Clin Invest 2001;108:203–13.
18. Tunny TJ, Jonsson JR, Klemm SA, Ballantine DM, Stowasser M, Gordon RD. Association of restriction fragment length polymorphism at the atrial natriuretic peptide gene locus with aldosterone responsiveness to angiotensin in aldosterone-producing adenoma. Biochem Biophys Res Commun 1994;204:1312–7.
19. Vesely DL. Atrial natriuretic peptides: anticancer agents. J Investig Med 2005;53:360–5.
20. Hellermann G, Kong X, Gunnarsdottir J, et al. Mechanism of bronchoprotective effects of a novel natriuretic hormone peptide. J Allergy Clin Immunol 2004;113:79–85.
21. Mohapatra SS, Lockey RF, Vesely DL, Gower WR, Jr. Natriuretic peptides and genesis of asthma: an emerging paradigm? J Allergy Clin Immunol 2004;114:520–6.
22. Schwartz AG, Prysak GM, Bock CH, Cote ML. The molecular epidemiology of lung cancer. Carcinogenesis 2007;28:507–18.
23. Martey CA, Pollock SJ, Turner CK, et al. Cigarette smoke induces cyclooxygenase-2 and microsomal prostaglandin E2 synthase in human lung fibroblasts: implications for lung inflammation and cancer. Am J Physiol Lung Cell Mol Physiol 2004;287:L981–91.
24. Knaapen AM, Borm PJ, Albrecht C, Schins RP. Inhaled particles and lung cancer. Part A: Mechanisms. Int J Cancer 2004;109:799–809.
25. Arenberg D. Chemokines in the biology of lung cancer. J Thorac Oncol 2006;1:287–8.
26. Pandey KN, Nguyen HT, Sharma GD, Shi SJ, Kriegel AM. Ligand-regulated internalization, trafficking, and down-regulation of guanylyl cyclase/atrial natriuretic peptide receptor-A in human embryonic kidney 293 cells. J Biol Chem 2002;277:4618–27.
27. Sun Y, Eichelbaum EJ, Wang H, Vesely DL. Atrial natriuretic peptide and long acting natriuretic peptide inhibit ERK 1/2 in prostate cancer cells. Anticancer Res 2006;26:4143–8.
28. Sun Y, Eichelbaum EJ, Wang H, Vesely DL. Vessel dilator and kaliuretic peptide inhibit ERK 1/2 activation in human prostate cancer cells. Anticancer Res 2006;26:3217–22.
29. Karin M. Mitogen activated protein kinases as targets for development of novel anti-inflammatory drugs. Ann Rheum Dis 2004;63 Suppl 2:ii62–4.
30. Greten FR, Eckmann L, Greten TF, et al. IKKβ links inflammation and tumorigenesis in a mouse model of colitis-associated cancer. Cell 2004;118:285–96.
31. Pikarsky E, Porat RM, Stein I, et al. NF-κB functions as a tumour promoter in inflammation-associated cancer. Nature 2004;431:461–6.
32. Massion PP, Carbone DP. The molecular basis of lung cancer: molecular abnormalities and therapeutic implications. Respir Res 2003;4:12.
33. Ahn KS, Sethi G, Aggarwal BB. Simvastatin potentiates TNF-α-induced apoptosis through the down-regulation of NF-κB-dependent antiapoptotic gene products: role of IκBα kinase and TGF-β-activated kinase-1. J Immunol 2007;178:2507–16.
34. Ashworth T, Roy AL. Cutting edge: TFII-I controls B cell proliferation via regulating NF-κB. J Immunol 2007;178:2631–5.
35. Inoue J, Gohda J, Akiyama T, Semba K. NF-κB activation in development and progression of cancer. Cancer Sci 2007;98:268–74.
36. Kim S, Millet I, Kim HS, et al. NF-κ B prevents β cell death and autoimmune diabetes in NOD mice. Proc Natl Acad Sci U S A 2007;104:1913–8.
37. Oka D, Nishimura K, Shiba M, et al. Sesquiterpene lactone parthenolide suppresses tumor growth in a xenograft model of renal cell carcinoma by inhibiting the activation of NF-κB. Int J Cancer 2007;120:2576–81.
38. Saccani A, Schioppa T, Porta C, et al. p50 nuclear factor-κB overexpression in tumor-associated macrophages inhibits M1 inflammatory responses and antitumor resistance. Cancer Res 2006;66:11432–40.
39. Vilimas T, Mascarenhas J, Palomero T, et al. Targeting the NF-κB signaling pathway in Notch1-induced T-cell leukemia. Nat Med 2007;13:70–7.
40. Schmidt D, Textor B, Pein OT, et al. Critical role for NF-κB-induced JunB in VEGF regulation and tumor angiogenesis. EMBO J 2007;26:710–9.
41. Vellaichamy E, Sommana NK, Pandey KN. Reduced cGMP signaling activates NF-κB in hypertrophied hearts of mice lacking natriuretic peptide receptor-A. Biochem Biophys Res Commun 2005;327:106–11.
42. Oliveira AM, Ross JS, Fletcher JA. Tumor suppressor genes in breast cancer: the gatekeepers and the caretakers. Am J Clin Pathol 2005;124 Suppl:S16–28.
43. Gabellini C, Del Bufalo D, Zupi G. Involvement of RB gene family in tumor angiogenesis. Oncogene 2006;25:5326–32.
44. Fluge T, Forssmann WG, Kunkel G, et al. Bronchodilation using combined urodilatin - albuterol administration in asthma: a randomized, double-blind, placebo-controlled trial. Eur J Med Res 1999;4:411–5.